

GLOBAL POLYNOMIAL LEVEL SETS FOR NUMERICAL DIFFERENTIAL GEOMETRY OF SMOOTH CLOSED SURFACES*

SACHIN KRISHNAN THEKKE VEETIL[†], GENTIAN ZAVALANI[‡], UWE HERNANDEZ ACOSTA[‡], IVO F. SBALZARINI^{†§}, AND MICHAEL HECHT^{¶¶}

Abstract. We present a computational scheme that derives a global polynomial level set parametrisation for smooth closed surfaces from a regular surface-point set and prove its uniqueness. This enables us to approximate a broad class of smooth surfaces by affine algebraic varieties. From such a global polynomial level set parametrisation, differential-geometric quantities like mean and Gauss curvature can be efficiently and accurately computed. Even 4th-order terms such as the Laplacian of mean curvature are approximated with high precision. The accuracy performance results in a gain of computational efficiency, significantly reducing the number of surface points required compared to classic alternatives that rely on surface meshes or embedding grids. We mathematically derive and empirically demonstrate the strengths and the limitations of the present approach, suggesting it to be applicable to a large number of computational tasks in numerical differential geometry.

Key words. Numerical differential geometry, surface approximation, mean curvature, Gauss curvature, level set, surface diffusion

MSC codes. 53Z50, 65D18

1. Introduction. Classic differential geometry of closed two-dimensional surfaces $S \subseteq \mathbb{R}^3$, $\partial S = \emptyset$, goes back to Carl Friedrich Gauss [22, 41], Bernhard Riemann [2, 38], and others. Numerically computing or approximating such surfaces' main geometric quantities, like *Gauss and mean curvature*, is of fundamental importance across scientific disciplines such as *biophysics* [48], *mechanics* [62, 66], *medical imaging* [39], *sociology* [26], and *computer graphics* [5, 78]. High accuracy of these approximations is key in many applications, including dynamic surface models where deformations are governed by the *intrinsic Laplacian of curvature* [71], *surface diffusion* [28, 74], and the *dynamics of cell membranes and vesicles* [67]. Such models that require accurate numerical computation of 4th-order differential terms, such as the Laplacian of mean curvature, present a challenge to available numerical methods.

We here address this challenge by combining algebraic geometry with classic numerical analysis in order to formulate a mathematical theory that enables us to approximate smooth closed surfaces $S \approx Q_S^{-1}(0)$ by algebraic varieties (i.e., hypersurfaces) with global polynomial level set (GPLS) parametrisation Q_S . As we demonstrate here, the GPLS can be numerically computed in an efficient way for a large class of surfaces. The GPLS can subsequently be used to compute geometric quantities with high precision, enabling efficient approximation of higher-order quantities.

2. Related work. The importance of the present computational challenge is manifest in the large number of previous works. Consequently, an exhaustive overview of the literature cannot be given here. Instead, we restrict ourselves to mentioning those contributions

*

Funding: This work was partially funded by the Center of Advanced Systems Understanding (CASUS), financed by Germany's Federal Ministry of Education and Research (BMBF) and by the Saxon Ministry for Science, Culture and Tourism (SMWK) with tax funds on the basis of the budget approved by the Saxon State Parliament.

[†]Technische Universität Dresden, Faculty of Computer Science, Dresden, Germany.

Max Planck Institute of Molecular Cell Biology and Genetics, Dresden, Germany.

Center for Systems Biology Dresden, Dresden Germany

[‡]Center for Advanced Systems Understanding (CASUS), Görlitz, Germany.

[§]Center for Scalable Data Analytics and Artificial Intelligence ScaDS.AI, Dresden, Germany.

^{¶¶}Corresponding author. Email: m.hecht@hzdr.de

that directly relate to or inspired our work. This includes methods where tracer points $P \subseteq S$ are placed on the surface in order to approximate S by *local interpolation* over finite neighbourhoods. Well-established interpolation methods include approaches based on *B-splines* [11, 12, 27], *Galerkin mesh-based* [59, 72] *finite element methods* [15, 17–20, 61], and triangulated surface methods [40].

Alternatively, surfaces can be approximated by a discrete or discretised implicit representation. This includes *level set methods* [50, 51, 68–70], *local kernel (radial basis function) parametrisations* [6, 7, 36, 52], *closest point methods* [43–45, 60], and *phase field methods* [55–57].

All of these approaches have in common that they approximate the surface with discrete points, meshes, or grids. Then, differential geometric quantities are computed on these discrete surface approximations using numerical methods. This introduces a second approximation, namely of the (surface) differential operators by their discretizations on the discrete surface approximation. This often prevents reaching the levels of accuracy required to compute higher-order geometric quantities.

The present approach avoids the second approximation by representing the surface globally as an algebraic variety. This leads to a surface representation that is continuous (even smooth) and defined everywhere, albeit supported on a finite set of discrete surface points. Doing so in a proper polynomial basis, we can compute any differential quantities to machine precision without introducing another approximation. While it has long been known that polynomial surface approximations have some desirable properties, and some methods have computed them piecewise, see e.g., [24, 53], we here exploit a recent advancement in polynomial interpolation [34] that allows us to compute such representations globally.

3. Main results. The GPLS method presented here determines a multivariate polynomial $Q_S(x)$, $x \in \mathbb{R}^3$, from points on a surface $P \subseteq S$ such that the surface is approximated by the zero-level set (zero contour) $S \approx Q_S^{-1}(0)$ of the polynomial. We do so for two classes of closed surfaces $S \subseteq \mathbb{R}^3$, $\partial S = \emptyset$:

- C1) algebraic varieties M of low degree: in this case the GPLS approach amounts to a *mesh-free particle method* that only relies on a *regular point set* $P \subseteq M$ sampled on the surface and does not require any surrounding (narrow band) grid or mesh.
- C2) non-algebraic surfaces S : in this case the GPLS approach amounts to fitting a global polynomial approximation of a given discretised (*relaxed*) *signed distance function* and yields an alternative classic level set redistancing methods [76, 77].

In both cases, $Q_M^{-1}(0)$ approximates (up to the interpolation or fitting error) the original surface by a uniquely determined algebraic variety, see Theorem 6.1(iv, v, vi). This means that regardless of whether the original surface was algebraic or not, the GPLS approximation of it always is. It also means that the exact same (unique) surface approximation is obtained from a given set of surface points P regardless of the maximum polynomial degree chosen. The unique polynomial approximation of the surface can then be used to accurately compute *mean and Gauss curvature* as well as their derivatives, e.g., the *Laplacian of mean curvature*, as we demonstrate in the numerical experiments of Section 9.

3.1. Notation. Let $m, n \in \mathbb{N}$, $p > 0$. Throughout this article, $\Omega = [-1, 1]^m$ denotes the m -dimensional *standard hypercube* and $C^0(\Omega, \mathbb{R})$ the *Banach space* of continuous functions $f : \Omega \rightarrow \mathbb{R}$ with norm $\|f\|_{C^0(\Omega)} = \sup_{x \in \Omega} |f(x)|$. We denote by $e_1 = (1, 0, \dots, 0), \dots, e_m = (0, \dots, 0, 1) \in \mathbb{R}^m$ the standard basis, by $\|\cdot\|_p$ the l_p -norm on \mathbb{R}^m , and by $\|M\|_p$ the l_p -norm of a matrix $M \in \mathbb{R}^{m \times m}$. Further, $A_{m,n,p} \subseteq \mathbb{N}^m$ denotes all multi-indices $\alpha = (\alpha_1, \dots, \alpha_m) \in \mathbb{N}^m$ with $\|\alpha\|_p \leq n$. We order $A_{m,n,p}$ with respect to the lexicographical order \preceq on \mathbb{N}^m going from the last entry to the first, e.g., $(5, 3, 1) \preceq (1, 0, 3) \preceq (1, 1, 3)$. We call A *downward closed* if and only if there is no $\beta = (b_1, \dots, b_m) \in \mathbb{N}^m \setminus A$ with $b_i \leq a_i, \forall i = 1, \dots, m$ for some

$\alpha = (a_1, \dots, a_m) \in A$ [9].

The sets $A_{m,n,p}$ are downward closed for all $m, n \in \mathbb{N}$, $p > 0$, and induce a generalised notion of *polynomial l_p -degree* as follows: We consider the *real polynomial ring* $\mathbb{R}[x_1, \dots, x_m]$ in m variables and denote by Π_m the \mathbb{R} -vector space of all real polynomials in m variables. For $A \subseteq \mathbb{N}^m$, $\Pi_A \subseteq \Pi_m$ denotes the *polynomial subspace* $\Pi_A = \text{span}\{x^\alpha\}_{\alpha \in A}$ spanned by the (unless further specified) *canonical* (monomial) *basis*. Choosing $A = A_{m,n,p}$ yields the spaces $\Pi_{A_{m,n,p}}$. The particular cases of *total degree* $A = A_{m,n,1}$, *Euclidean degree* $A = A_{m,n,2}$, and *maximum degree* $A = A_{m,n,\infty}$ will play an important role for the polynomial approximation quality. As noticed by [79], the sizes of these sets scale polynomially, sub-exponentially, and exponentially with dimension, respectively:

$$(3.1) \quad |A_{m,n,1}| = \binom{m+n}{n} \in \mathcal{O}(m^n), \quad |A_{m,n,2}| \approx \frac{(n+1)^m}{\sqrt{\pi m}} \left(\frac{\pi e}{2m}\right)^{m/2} \in o(n^m), \quad |A_{m,n,\infty}| = (n+1)^m.$$

Given linear ordered sets $A \subseteq \mathbb{N}^m$, $B \subseteq \mathbb{N}^n$, we slightly abuse notation by writing matrices $R_{A,B} \in \mathbb{R}^{|A| \times |B|}$ as

$$(3.2) \quad R_{A,B} = (r_{\alpha,\beta})_{\alpha \in A, \beta \in B} \in \mathbb{R}^{|A| \times |B|},$$

where $r_{\alpha,\beta} \in \mathbb{R}$ is the α -th, β -th entry of $R_{A,B}$. Finally, we use the standard *Landau symbols* $f \in \mathcal{O}(g) \iff \limsup_{x \rightarrow \infty} \frac{|f(x)|}{|g(x)|} \leq \infty$, $f \in o(g) \iff \lim_{x \rightarrow \infty} \frac{|f(x)|}{|g(x)|} = 0$.

4. Unisolvent nodes and multivariate interpolation. We briefly summarise here the essential concepts from [8, 9, 31–34] on which our approach rests, in particular the notion of unisolvence with respect to generalised polynomial degree.

4.1. The notion of unisolvence. For a downward closed multi-index set $A \subseteq \mathbb{N}^m$, $m \in \mathbb{N}$, and the induced polynomial space Π_A , a set of nodes $P \subseteq \Omega$ is called *unisolvence with respect to Π_A* if and only if there exists no hypersurface $H = Q^{-1}(0)$ generated by a polynomial $0 \neq Q \in \Pi_A$ with $P \subseteq H$. The opposite notion of non-unisolvent nodes P allows us to derive global polynomial hypersurfaces $Q_S^{-1}(0) \supseteq P$ that contain a given (regular) point set $P \subseteq S$ and approximate the initial surface S , see Section 5. The following concepts are useful in the derivation:

DEFINITION 4.1 (1st and 2nd essential assumptions). *Let $m \in \mathbb{N}$, $A \subseteq \mathbb{N}^m$ be a downward closed set of multi-indices, and $\Pi_A \subseteq \Pi_m$ the polynomial sub-space induced by A . We consider the generating nodes given by the grid*

$$(4.1) \quad \text{GP} = \bigoplus_{i=1}^m P_i, \quad P_i = \{p_{0,i}, \dots, p_{n_i,i}\} \subseteq \mathbb{R}, \quad n_i = \max_{\alpha \in A}(\alpha_i),$$

$$(4.2) \quad P_A = \{(p_{\alpha_1,1}, \dots, p_{\alpha_m,m}) : \alpha \in A\}.$$

A1) *If the $P_i \subseteq [-1, 1]$ are arbitrary distinct points then the node set P_A is said to satisfy the 1st essential assumption.*

A2) *We say that the 2nd essential assumption holds if in addition the P_i are chosen as the Chebyshev-Lobatto nodes that, in addition, are Leja-ordered [42], i.e.,*

$$P_i = \{p_0, \dots, p_n\} = \pm \text{Cheb}_n = \left\{ \cos\left(\frac{k\pi}{n}\right) : 0 \leq k \leq n \right\}$$

and the following holds

$$(4.3) \quad |p_0| = \max_{p \in P} |p|, \quad \prod_{i=0}^{j-1} |p_j - p_i| = \max_{j \leq k \leq m} \prod_{i=0}^{j-1} |p_k - p_i|, \quad 1 \leq j \leq n.$$

Note that $\{p_0, p_1\} = \{-1, 1\}$ for all Leja-ordered Chebyshev-Lobatto nodes Cheb_n with $n \geq 1$. Points P_A that fulfil the *1st essential assumption* form non-tensorial (non-symmetric) grids and are unisolvent with respect to Π_A [8, 9, 31–34]. This allows generalising classic interpolation approaches to higher dimensions.

4.2. Multivariate Newton and Lagrange interpolation. Given unisolvent nodes P_A , multivariate generalisations of the classic 1D Newton and Lagrange interpolation schemes can be derived, see e.g., [34, 47]:

DEFINITION 4.2 (Multivariate Lagrange polynomials). *Let $m \in \mathbb{N}$, $A \subseteq \mathbb{N}^m$ be a downward closed set of multi-indices, $P_A \subseteq \Omega$ be a set of unisolvent nodes satisfying (A1) from Definition 4.1, and $\Pi_A = \text{span}\{x^\alpha\}_{\alpha \in A} \subseteq \Pi_m$ be the corresponding canonical polynomial space. We define the multivariate Lagrange polynomials $L_\alpha \in \Pi_A$ by*

$$(4.4) \quad L_\alpha(p_\beta) = \delta_{\alpha,\beta},$$

where $\delta_{\cdot,\cdot}$ is the Kronecker delta.

Since the $|A|$ -many Lagrange polynomials are linearly independent functions, and $\dim \Pi_A = |A|$, the Lagrange polynomials are a basis of Π_A . Consequently, any function $f : \Omega \rightarrow \mathbb{R}$ possesses a unique interpolant $Q_{f,A} \in \Pi_A$ with $Q_{f,A}(p_\alpha) = f(p_\alpha) \forall \alpha \in A$, given by

$$(4.5) \quad Q_{f,A}(x) = \sum_{\alpha \in A} f(p_\alpha) L_\alpha(x), \quad x \in \mathbb{R}^m.$$

However, this does not allow for efficient evaluation of $Q_{f,A}$ at an argument $x_0 \notin P_A \subseteq \mathbb{R}^m$. For that, the Newton basis of Π_A is better suited:

DEFINITION 4.3 (Multivariate Newton polynomials). *Let $m \in \mathbb{N}$, $A \subseteq \mathbb{N}^m$ be a downward closed set of multi-indices, $P_A \subseteq \Omega$ be a set of unisolvent nodes satisfying (A1) from Definition 4.1. Then, the multivariate Newton polynomials are given by*

$$(4.6) \quad N_\alpha(x) = \prod_{i=1}^m \prod_{j=0}^{\alpha_i-1} (x_i - p_{j,i}), \quad \alpha \in A,$$

where $p_{j,i} \in P_i$ from Eq. (4.1).

In dimension $m = 1$, both of these definitions reduce to the classic definitions of Lagrange and Newton polynomials, see e.g., [23, 75, 80]. In arbitrary dimensions, efficient algorithms exist for computing the interpolant in Newton form as well as for its evaluation at any argument $x_0 \in \mathbb{R}^m$ and its differentiation, see [35].

5. The dual notion of unisolvence. For the purpose of surface approximation, we use the dual notion of unisolvence. Rather than asking for nodes $P \subseteq \mathbb{R}^m$, $m \in \mathbb{N}$, that are unisolvent with respect to a given polynomial space Π , already [13, 14] asked the dual question of finding a polynomial space Π with respect to which a given set of points $P \subseteq \Omega$ is unisolvent. We here formulate this question in a generalised way.

5.1. Unisolvent polynomial spaces. In order to formulate the dual notion of unisolvence, it is useful to consider the *Grassmann manifold* $\text{Gr}(k, X)$, i.e., the smooth manifold that consists of all k -dimensional subspaces of the vector space X [49]. In particular, $\text{Gr}(1, \mathbb{R}^m) = \mathbb{R}\mathbb{P}^{m-1}$ and $\text{Gr}(1, \mathbb{C}^m) = \mathbb{C}\mathbb{P}^{m-1}$ are the real and complex *projective spaces*, respectively [16, 30]. Using this notion, we state:

THEOREM 5.1. *Let $m, k \in \mathbb{N}$, $\mathcal{P}_k = \{P \subseteq \mathbb{R}^m : |P| = k\}$ be the set of all subsets of \mathbb{R}^m of cardinality k , and $X = \Pi_{m,k-1,\infty}$ the space of all polynomials with l_∞ -degree at most $k-1$. Then, there is one and only one polynomial subspace $\Pi_P \subseteq X$ of dimension $\dim \Pi_P = k$ such that P is unisolvent with respect Π_P . In particular, the map*

$$(5.1) \quad \Gamma_k : \mathcal{P}_k \longrightarrow \text{Gr}(k, X), \quad P \in \mathcal{P}_k \text{ is unisolvent with respect to } \Gamma_k(P), \quad X = \Pi_{m,k-1,\infty},$$

is well-defined and smooth.

For $m = 1$ we have $X = \Pi_{m,k-1,\infty} = \Pi_{1,k-1,1}$ and $\text{Gr}(k, X) = X$. Since k distinct nodes are unisolvent in dimension 1 with respect to X , Theorem 5.1 becomes trivial, and $\Gamma_k(P) \equiv X$ is constant in that case.

Proof. According to (A1) from Definition 4.1, we choose unisolvent nodes $P_{A_{m,k-1,\infty}}$ with respect to $X = \Pi_{m,k-1,\infty}$, $\dim X = k^m$, and denote by $L_\alpha \in X$, $\alpha \in A_{m,k-1,\infty}$, the corresponding Lagrange basis. We fix an ordering $P = \{p_1, \dots, p_k\}$ and consider the corresponding Vandermonde matrix

$$(5.2) \quad R_{A,P} = (r_{i,\alpha}) \in \mathbb{R}^{|P| \times k^m}, \quad r_{i,\alpha} = L_\alpha(p_i), \quad i = 1, \dots, |P|, \alpha \in A_{m,k-1,\infty}.$$

Let $\mu = \text{rank}(R_{A,P}) \leq |P| = k$ be the rank of R and $D = \text{diag}(\overbrace{1, \dots, 1}^\mu, \overbrace{0, \dots, 0}^{k-\mu}) \in \mathbb{R}^{k \times k}$ the diagonal matrix with the first μ entries equal to 1 and all others equal to 0. Let further $C \in \mathbb{R}^{k^m \times k}$ be a solution of $RC = D$ and $C_i = (c_{\alpha,i}) \in \mathbb{R}^{k^m}$ be the i -th column of C . Then

$$\mathcal{L}_i(x) = \sum_{\alpha \in A_{m,k-1,\infty}} c_{\alpha,i} L_\alpha(x) \in X, \quad i = 1, \dots, \mu$$

yields Lagrange polynomials with $\mathcal{L}_i(p_j) = \delta_{i,j}$, $1 \leq j \leq \mu$, where $\delta_{\cdot,\cdot}$ denotes the Kronecker delta. Thus, the \mathcal{L}_i are linearly independent.

We argue by contradiction to show that $\mu = k$. Indeed, if $\mu < k$ then there is no polynomial $Q \in \Pi_{A_{m,k-1,\infty}}$ with $Q(p_j) = 0 \forall j = 1, \dots, \mu$ and $Q(p_l) = 1$ for $l > \mu$. We denote by $p_j = (p_{j,i})_{i=1,\dots,m} \in P \subseteq \mathbb{R}^m$ the coordinates of the p_j , $1 \leq j \leq k$. Then, there is a sequence p_{j,i_j} , $1 \leq i_j \leq m$, of coordinate entries such that $p_{l,i_l} \neq p_{j,i_j}$ for all $1 \leq j \leq \mu$. Consequently, setting

$$Q(x) = \frac{\prod_{j=1}^\mu (x_{i_j} - p_{j,i_j})}{\prod_{j=1}^\mu (p_{l,i_l} - p_{j,i_j})} \in \Pi_{A_{m,\mu,\infty}} \subseteq \Pi_{m,k-1,\infty}, \quad l > \mu$$

provides such a polynomial, contradicting $\mu < k$. Thus, setting $\mathfrak{m}(P) := \{Q \in X : Q(p) = 0 \forall p \in P\}$ implies that

$$\Gamma_k(P) := X / \mathfrak{m}(P) \cong \text{span}(\mathcal{L}_i)_{i=1,\dots,\mu}$$

is the uniquely determined polynomial subspace for which P is unisolvent. Since $\text{Gr}(k, X)$ is a smooth manifold [49], and the \mathcal{L}_i depend smoothly on P , this shows that $\Gamma_k : \mathcal{P}_k \longrightarrow \text{Gr}(k, X)$ is a well-defined smooth map. \square

Theorem 5.1 guarantees that the algebraic variety $M = Q_M^{-1}(0)$ we derive as GPLS from given points $P \subseteq S$ is uniquely determined.

6. Algebraic varieties and polynomial hypersurfaces. Formulating the practical consequences of Theorem 5.1 relies on concepts from algebraic geometry. An excellent overview of these topics is given by [29]. We start by stating:

THEOREM 6.1. *Let $m \in \mathbb{N}$, $A \subseteq \mathbb{N}^m$ be a downward closed set of multi-indices, $P_A \subseteq \Omega$ be a set of unisolvent nodes satisfying (A1) from Definition 4.1. Denote by $\{L_\alpha\}_{\alpha \in A} \subseteq \Pi_A$ the Lagrange basis with respect to Π_A and P_A . Let further Γ_k be as in Theorem 5.1. Given any set of points $P \subseteq \mathbb{R}^m$, the following holds:*

- i) *There is a set $P_0 \subseteq P$ of maximum cardinality $k = |P_0|$, which can be determined in $\mathcal{O}(|A|^3)$ operations, such that $\Gamma_k(P_0) \subseteq \Pi_A$.*
- ii) *A Lagrange basis $\{\mathcal{L}_1, \dots, \mathcal{L}_k\} \subseteq \Gamma_k(P_0)$ with $\mathcal{L}_i(p_j) = \delta_{i,j}$, $1 \leq (i, j) \leq k$, $p_j \in P_0$, and a basis $\{\mathcal{M}_1, \dots, \mathcal{M}_{|A|-k}\} \subseteq \Pi_A/\Gamma_k(P_0)$ of the quotient space can be computed in $\mathcal{O}(|A|^3)$ operations.*
- iii) *Consider the affine algebraic variety $M = Q_M^{-1}(0)$ given by the polynomial hypersurface*

$$(6.1) \quad Q_M(x) = \sum_{i=1}^k \mathcal{L}_i(x) - 1.$$

Further, let $\mathfrak{m}_M = \{Q \in \Pi_A : Q(x) = 0 \forall x \in M\}$ be the vector space of polynomials identically vanishing on M , and $\Pi_M = \{Q|_M : Q \in \Pi_A\}$ be the vector space of polynomials restricted to M . Then

$$(6.2) \quad \Pi_M \cong \Pi_A/\mathfrak{m}_M \cong \Gamma_k(P_0).$$

- iv) *If $P \subseteq M = Q_M^{-1}(0)$, with Q_M from Eq. (6.1), then M and Q_M are uniquely determined up to adding polynomials from \mathfrak{m}_M , i.e. for any other maximal set $P_0 \neq P'_0 \subseteq P$, $|P_0| = |P'_0| = k$, with $\Gamma_k(P'_0) \subseteq \Pi_A$ there holds*

$$(6.3) \quad \Gamma_k(P'_0) = \Gamma_k(P_0) \quad \text{and} \quad Q_M(x) - Q_{M'}(x) = \sum_{i=1}^k \mathcal{L}_i(x) - \sum_{i=1}^k \mathcal{L}'_i(x) \in \mathfrak{m}_M,$$

where $\{\mathcal{L}'_i\}_{i=1, \dots, k}$ denotes the Lagrange basis from ii) with respect to P'_0 , and \mathfrak{m}_M is as in iii).

- v) *Let $A_1 \subseteq A_2 \subseteq \mathbb{N}^m$ be two choices of multi-index sets and P_{A_1}, P_{A_2} the corresponding unisolvent nodes fulfilling the assumptions of the theorem such that $P \subseteq M_1 = Q_{M_1}^{-1}(0)$ and $P \subseteq M_2 = Q_{M_2}^{-1}(0)$ holds for the corresponding level sets. Then, the two algebraic varieties are identical $M_1 = M_2$.*
- vi) *Let P_1 and P_2 be two sets of points and $P_1 \subseteq M_1 = Q_{M_1}^{-1}(0)$, $P_2 \subseteq M_2 = Q_{M_2}^{-1}(0)$, $Q_{M_1} \in \Pi_{A_1}$, $Q_{M_2} \in \Pi_{A_1}$, the (due to (v)) uniquely determined) corresponding algebraic varieties. If $P_1 \cup P_2 \subseteq M_1 \cap M_2$, then $M_1 = M_2$ are identical.*

Proof. If P is unisolvent with respect to Π_A , the statement is trivial. For non-unisolvent P all statements follow from the following observation: We order the nodes $P = \{p_1, \dots, p_{|P|}\}$ and consider the corresponding Vandermonde matrix, as in Eq. (5.2),

$$(6.4) \quad R_{A,P} = (r_{i,\alpha}) \in \mathbb{R}^{|P| \times |A|}, \quad r_{i,\alpha} = L_\alpha(p_i), \quad 1 \leq i \leq |P|, \alpha \in A.$$

By using *Gaussian elimination with full pivoting* (GEFP), see, e.g., [81], we can find a *LU*-decomposition of $R_{A,P}$. That is, there are *permutation matrices* $W_1 \in \mathbb{R}^{|P| \times |P|}$, $W_2 \in \mathbb{R}^{|A| \times |A|}$, a *unitary lower triangular matrix* $L \in \mathbb{R}^{|P| \times |A|}$, and an *upper triangular matrix* $U \in \mathbb{R}^{|A| \times |A|}$ such that

$$(6.5) \quad W_1 R_{A,P} W_2 = LU \quad \text{with} \quad U = \begin{pmatrix} U_1 & U_2 \\ 0 & 0 \end{pmatrix} \in \mathbb{R}^{l \times l}, U_1 \in \mathbb{R}^{k \times k}, U_2 \in \mathbb{R}^{k \times |A|-k}$$

and the k diagonal entries of U_1 do not vanish. Consequently, $\text{rank}(R_{A,P}) = \text{rank}(U) = \text{rank}(U_1) = k \in \mathbb{N}$. Let $P_0 = \{p_1, \dots, p_k\}$ be the first k nodes of the node set P when reordered according to W_1 , and denote by $L_{\beta_j} \in \Pi_A$, $1 \leq j \leq |A|$, the Lagrange polynomials with respect to Π_A and P_A when reordered according to W_2 . Denote by $S_{A,P} \in \mathbb{R}^{k \times |A|}$ the matrix given by the first k rows of $R_{A,P}$. Then, the Lagrange polynomials \mathcal{L}_i , $i = 1, \dots, k$, are uniquely determined as

$$(6.6) \quad \mathcal{L}_i(x) = \sum_{j=0}^{|A|} c_{ij} L_{\beta_j}(x) \quad \text{with} \quad C_i = (c_{ij})_{1 \leq j \leq |A|} \in \mathbb{R}^{|A|} \quad \text{solving} \quad S_{A,P} C_i = e_i,$$

where e_i is the i -th standard basis vector of \mathbb{R}^k . Since $\text{rank}(R_{A,P}) = k$, the set P_0 is the maximal subset of P with that property, yielding (i).

For the second claim, consider $D_j = (d_{j,i})_{i=1, \dots, k} \in \mathbb{R}^k$, $1 \leq j \leq |A| - k$, with

$$U_1 D_j = -U_2 e_j,$$

where e_j is the j -th standard basis vector of $\mathbb{R}^{|A|-k}$. Setting $(d_{j,i})_{i=1, \dots, |A|} := (D_j, -e_j) \in \mathbb{R}^{|A|}$ yields polynomials

$$(6.7) \quad \mathcal{M}_j(x) = \sum_{i=1}^{|A|} d_{j,i} L_{\beta_j}(x)$$

that form a basis of $\mathfrak{m}_M = \{Q \in \Pi_A : Q(P) = 0\} \cong \Pi_A / \Gamma_k(P_0)$. Therefore, the computational costs for solving Eqs. (6.5), (6.6), and (6.7) are all contained in $\mathcal{O}(|A|^3)$, proving (ii).

We use the fact that $\Gamma_k(P_0) \cong \text{span}\{\mathcal{L}_i\}_{i=1, \dots, k}$, which has already been proven in Eq. (6.6), to show (iii). Indeed, we observe that $P_0 \subseteq M$. Thus, the restricted Lagrange polynomials remain linearly independent, and because $\text{span}\{\mathcal{L}_{iM}\}_{i=1, \dots, k} \subseteq \Pi_M$ we obtain $\dim \Pi_M \geq \dim \Gamma_k(P_0) = k$. Consequently,

$$\Pi_A = \text{span}\{\mathcal{L}_i\}_{i=1, \dots, k} + \text{span}\{\mathcal{M}_i\}_{i=1, \dots, |A|-k} \cong \Gamma_k(P_0) + \mathfrak{m}_M$$

yields

$$\Gamma_k(P_0) \cong \Pi_A / \mathfrak{m}_M \supseteq \{Q_M : Q \in \Pi_A / \mathfrak{m}_M\} \cong \{Q_M : Q \in \Pi_A\} = \Pi_M$$

and therefore $\Gamma_k(P_0) \cong \Pi_M$, as claimed in (iii).

We prove (iv) by using a classic bases exchange argument [46]: We choose $p \in P'_0 \setminus P_0$. Since $P'_0 \subseteq Q_M^{-1}(0)$ and $Q_M(x) = \sum_{i=1}^k \mathcal{L}_i(x) - 1 = 0$, $\forall x \in M$, there exists a Lagrange polynomial \mathcal{L}_{i_0} , $1 \leq i_0 \leq k$, with $\mathcal{L}_{i_0}(p) \neq 0$. We then set

$$\mathcal{L}_{i_0}^1(x) = \frac{1}{\mathcal{L}_{i_0}(p)} \mathcal{L}_{i_0}(x) \in \Gamma_k(P_0) \quad \text{and} \quad \mathcal{L}_i^1(x) = \mathcal{L}_i(x) - \mathcal{L}_i(p) \mathcal{L}_{i_0}^1(x) \in \Gamma_k(P_0), \quad i \neq i_0.$$

Then exchange p_{i_0} with p , i.e., set $P_0^1 = (P_0 \setminus \{p_{i_0}\}) \cup \{p\} = \{p_i^1\}_{i=1, \dots, k}$ and observe that $\mathcal{L}_i^1(p_j^1) = \delta_{i,j}$, $\forall 1 \leq (i, j) \leq k$. Thus, we have constructed a Lagrange basis $\{\mathcal{L}_i^1\}_{i=1, \dots, k} \subseteq \Gamma_k(P_0)$ w.r.t. P_0^1 , implying that $\Gamma_k(P_0) = \Gamma_k(P_0^1)$, and therefore P_0^1 is unisolvent w.r.t. $\Gamma_k(P_0)$. Setting $Q_{M'}(x) = \sum_{i=1}^k \mathcal{L}_i^1(x)$ yields $Q_{M'}(p_i^1) = 1$ for all $i = 1, \dots, k$, implying $Q_{M'}(x) = Q_M(x) \equiv 0 \forall x \in M$. Thus, $Q_M(x) - Q_{M'}(x) \in \mathfrak{m}_M$ holds due to (iii). By recursively continuing this exchange procedure (at most k times), we construct a Lagrange basis $\{\mathcal{L}_i^k\}_{i=1, \dots, k}$ with respect to $P'_0 = P_0^k$ within $\Gamma_k(P_0)$ that satisfies Eq. (6.3), proving (iv).

(v) follows from observing that because $A_1 \subseteq A_2$ we have $\Pi_{A_1} \subseteq \Pi_{A_2}$. Hence, $Q_{M_1} \in \Pi_{A_2}$ and $Q_{M_1}(p) = Q_{M_2}(p) = 0$, $\forall p \in P$ imply that $Q_{M_1} - Q_{M_2} \in \mathfrak{m}_{M_2}$ due to (iii). Thus, $M_2 \subseteq$

$Q_{M_1}^{-1}(0) = M_1$. Vice versa, projecting Q_{M_2} onto Π_{M_1} yields $Q_{M_2} = \sum_{i=1}^k \mathcal{L}_i - 1 = Q_{M_1}$ with \mathcal{L}_i the Lagrange basis spanning Π_{M_1} . Hence, $Q_{M_2} - Q_{M_1} \in \Pi_{A_2}/\mathfrak{m}_{M_1}$ and thereby $M_1 \subseteq M_2$, proving the statement. Finally, (vi) follows directly from (iv) and (v). \square

Remark 6.2 (Uniqueness of the GPLS). We want to emphasise the importance of Theorem 6.1(iv, v, vi) stating that regardless of the choice of polynomial degree, $A_1 = A_{m,n_1,p_1}$, $A_2 = A_{m,n_2,p_2}$, $n_1 \leq n_2$, and of the points $P_1, P_2 \subseteq S$, the algebraic variety $M = M_1 = M_2$ is uniquely determined whenever $A_1 \subseteq A_2$ and $P_1 \cup P_2 \subseteq M_1 \cap M_2$. Therefore, the approximation of any closed smooth surface $S \subseteq \mathbb{R}^3$ by an algebraic variety $S \approx M = Q_M^{-1}(0)$ is uniquely determined by the point set $P \subseteq S \cap M$ in that sense.

DEFINITION 6.3 (Regular samples). *Given an algebraic variety $M = Q_M^{-1}(0) \subseteq \mathbb{R}^3$ with $Q_M \in \Pi_{A_{m,n,p}}$ of l_p -degree at most $n \in \mathbb{N}$, we call a point set $P \subseteq M$ regular if and only if there exists a subset $P_0 \subseteq P$ with $|P_0| = k \in \mathbb{N}$ and $\Gamma_k(P_0) = \Pi_M$ from Eq. (6.2).*

Since the associated matrix $R_{A,P}$, Eq. (6.4), has full rank with probability 1 for any uniformly random points $P \subseteq S$ [63, 73], one can expect P to be regular in practice whenever P is of sufficient size.

6.1. Global polynomial level sets for affine algebraic varieties. Using the statements of Theorem 6.1, we provide a numerical method for determining the GPLS approximation of a given affine algebraic variety, hence detailing contribution (C1) announced in the introduction. A GPLS for an affine algebraic variety of sufficiently low degree can be given by:

COROLLARY 6.4. *Let the assumptions of Theorem 6.1 be fulfilled, the bases $\{\mathcal{L}_1, \dots, \mathcal{L}_k\} \subseteq \Gamma_k(P_0)$, $\{\mathcal{M}_1, \dots, \mathcal{M}_{|A|-k}\} \subseteq \Pi_A/\Gamma_k(P_0)$ from Theorem 6.1(ii) be computed, $R_{A,P} \in \mathbb{R}^{|P| \times |A|}$ as in Eq. (6.4), M as in Theorem 6.1(iii), and Q_M as in Eq. (6.1).*

- i) *If $k = 1$ then $M = \mathcal{M}_1^{-1}(0)$ and $Q_M = \lambda \mathcal{M}_1$ for some $\lambda \in \mathbb{R} \setminus \{0\}$.*
- ii) *Let $f : \Omega \rightarrow \mathbb{R}$ be a (continuous) function. Then, the Lagrange interpolant*

$$(6.8) \quad Q_{f,P_0,A} = \sum_{i=1, \dots, k} f(p_i) \mathcal{L}_i \in \Pi_M$$

is uniquely determined in $\Pi_M \cong \Gamma_k(P_0)$ from Eq. (6.2).

Proof. The proof follows directly from Theorem 6.1 and from the existence of optimal solutions to least squares problems, see e.g., [81]. \square

Remark 6.5. In the special case of Corollary 6.4(i), the GPLS of M is straightforwardly computed by deriving \mathcal{M}_1 according to Eq. (6.7). In Section 9, we numerically demonstrate that this approach provides an effective scheme for this class of surfaces.

Remark 6.6. Consider the solution to the least squares problem

$$(6.9) \quad C = (c_\alpha)_{\alpha \in A} = \operatorname{argmin}_{X \in \mathbb{R}^{|A|}} \{ \|R_{A,P}X - F\|_2^2 \}$$

with $F = (f(p_i))_{i=1, \dots, k} \in \mathbb{R}^{|P|}$. Then $f \approx Q_{P,f,A} = \sum_{\alpha \in A} c_\alpha L_\alpha \in \Pi_A$. Moreover, up to the regression error, we have $Q_{P,f,A} - Q_{f,P_0,A} \in \mathfrak{m}_M$ with $Q_{f,P_0,A}$ from Eq. (6.8) and \mathfrak{m}_M as in Theorem 6.1(iii). Thus, in practice, it might be more convenient to derive the regressor $Q_{P,f,A}$ instead of the interpolant $Q_{f,P_0,A}$.

6.2. Global polynomial level sets for non-algebraic surfaces. For non-algebraic surfaces $S \subseteq \mathbb{R}^3$, the matrix $R_{A,P} \in \mathbb{R}^{|P| \times |A|}$ in Eq. (6.4) does not (sharply) numerically separate into kernel (null space) and co-kernel. This makes direct computation of the bases $\{\mathcal{L}_1, \dots, \mathcal{L}_k\} \subseteq \Gamma_k(P_0)$, $\{\mathcal{M}_1, \dots, \mathcal{M}_{|A|-k}\} \subseteq \Pi_A/\Gamma_k(P_0)$ practically impossible. To resolve the issue, we introduce:

DEFINITION 6.7 (Relaxed signed distance function).

Let $S \subseteq \mathbb{R}^3$ be a smooth closed surface, $P \subseteq S$ be a set of points on the surface, and $P_D = P_D^+ \cap P_D^- \subseteq \Omega \setminus S$ arbitrary points in some vicinity of S to either side of the surface. Given a smooth and strictly positive function $\mu : \Omega \rightarrow \mathbb{R}^+$, we call

$$(6.10) \quad d(x) = \begin{cases} \mu(x) \text{dist}(x, M) & \text{if } x \in P_D^+ \\ -\mu(x) \text{dist}(x, M) & \text{if } x \in P_D^- \\ 0 & \text{if } x \in P \subseteq M \end{cases}$$

a relaxed signed distance function with respect to P_D , where the relaxation factor $\mu(x)$ reflects the deviation from the proper signed-distance function.

Remark 6.8. Given a flat surface triangulation, see e.g., [59, 72], of the surface $S \subseteq \mathbb{R}^3$, a point set P_D as described above can be generated by moving the vertices $V = P$ of the triangles along the mesh-normal field η , i.e., $q \in P \mapsto q + D_q \eta = q'$, $D_q \in \mathbb{R} \setminus \{0\}$. Setting $d(q') = D_q$ yields a relaxed signed distance function as defined above.

Given a relaxed signed distance function with respect to P_D , we consider the node set $\bar{P} = P \cup P_D$ and extend $R_{A,P}$ in Eq. (6.4) to $\bar{R}_{A,P} = (r_{i,\alpha})_{i=1,\dots,|\bar{P}|,\alpha \in A} \in \mathbb{R}^{|\bar{P}| \times |A|}$ with $r_{i,\alpha} = L_\alpha(p_i)$, $p_i \in \bar{P}$. The coefficients $C_A = (c_\alpha)_{\alpha \in A}$ of a polynomial $Q_d \in \Pi_A$

$$(6.11) \quad Q_d(x) = \sum_{\alpha \in A} c_\alpha L_\alpha(x) \approx d(x)$$

approximating the relaxed signed distance function can be derived by solving the least squares problem

$$C_A = \operatorname{argmin}_{X \in \mathbb{R}^{|A|}} \{ \|\bar{R}_{A,P} X - D\|_2^2 \}, \quad D = (d(p_i))_{i=1,\dots,|\bar{P}|}.$$

Level-set methods are most conveniently formulated in terms of the signed-distance function [76, 77]. Here, we use a relaxed version to derive a GPLS $S \approx Q_d^{-1}(0)$ with non-vanishing gradient, i.e.,

$$(6.12) \quad \nabla Q_d(x) \neq 0 \quad \text{for all } x \in Q_d^{-1}(0).$$

If the approximation $S \approx S' = Q_d^{-1}(0)$ is sufficiently close, the polynomial normal field $\eta = \nabla Q_d / \|\nabla Q_d\|$ enables computing geometric entities of S' with high (machine) precision, as demonstrated in Section 9.4. The approximation quality, however, depends on the approximation power of the regression scheme, as addressed in the following section.

7. Approximation theory. The above computational schemes derive GPLS approximations to algebraic varieties M and non-algebraic surfaces S from a regular surface point set $P \subseteq M$ using the statements of Theorem 6.1. If non-polynomial surfaces $S \subseteq \mathbb{R}^3$ are to be approximated, however, the question arises of how accurate the GPLS approximation is. We address this question by using:

DEFINITION 7.1 (Lebesgue constant). Let $m \in \mathbb{N}$, $A \subseteq \mathbb{N}^m$ be a downward closed set of multi-indices, $P_A \subseteq \Omega$ be a set of unisolvent nodes satisfying (A1) from Definition 4.1. Let $f \in C^0(\Omega, \mathbb{R})$ and $Q_{f,A}(x) = \sum_{\alpha \in A} f(p_\alpha) L_\alpha(x)$ be its Lagrange interpolant. Then, we define the Lebesgue constant analogously to the 1D case, see e.g. [23], as

$$\Lambda(P_A) := \sup_{f \in C^0(\Omega, \mathbb{R}), \|f\|_{C^0(\Omega)} \leq 1} \|Q_{f,A}\|_{C^0(\Omega)} = \left\| \sum_{\alpha \in A} |L_\alpha| \right\|_{C^0(\Omega)}.$$

Based on the 1D estimate

$$(7.1) \quad \Lambda(\text{Cheb}_n) = \frac{2}{\pi} (\log(n+1) + \gamma + \log(8/\pi)) + \mathcal{O}(1/n^2),$$

known for Chebyshev-Lobatto nodes, surveyed by [4], [8, 9, 32] further detail and study this concept in mD and show that unisolvent nodes satisfying (A2) from Definition 4.1 induce high approximation power reflected in the small corresponding Lebesgue constants. Motivated by the classic Lebesgue inequality [4], we deduce the following bound on the approximation error of the present regression scheme:

THEOREM 7.2. *Let the assumptions of Theorem 6.1(i–iv) be fulfilled and $M \subseteq \Omega$ be as in Theorem 6.1(iii); let further $P_{A_{m,n,p}}$, $n, m \in \mathbb{N}$, $p > 0$ be unisolvent nodes satisfying (A1) from Definition 4.1, $f : \Omega \rightarrow \mathbb{R}$ be a continuous function, and $f|_M : M \rightarrow \mathbb{R}$ its restriction to M . We denote by $Q_{f,A_{m,n,p}} = \sum_{\alpha \in A_{m,n,p}} f(p_\alpha) L_\alpha \in \Pi_{A_{m,n,p}}$ the Lagrange interpolant of f in $P_{A_{m,n,p}}$ and by*

$$Q_{f,P_0,A_{m,n,p}} = \sum_{i=1,\dots,k} f(p_i) \mathcal{L}_i \in \Pi_M$$

the polynomial interpolant of f in P_0 according to Corollary 6.4(ii). Then, the approximation error is bounded by

$$(7.2) \quad \|f|_M - Q_{f,P_0,A_{m,n,p}}\|_{C^0(M)} \leq (1 + \Lambda(P_A) \|S_{A,P}\|_\infty) \|f - Q_{f,A}\|_{C^0(\Omega)} + \mu \Lambda(P_A) \|S_{A,P}\|_\infty,$$

where $S_{A_{m,n,p},P_0} \in \mathbb{R}^{|A_{m,n,p}| \times |P_0|}$ with $S_{A_{m,n,p},P_0} R_{A_{m,n,p},P_0} = \text{Id}_{\mathbb{R}^{|A_{m,n,p}| \times |A_{m,n,p}|}}$ is the Moore–Penrose pseudo-left-inverse, see e.g., [1, 81] of the regression matrix $R_{A_{m,n,p},P_0}$ from Eq. (6.4) and

$$\mu = \|\tilde{F} - F\|_\infty, \quad \tilde{F} = (Q_{f,P_0,A}(p_i))_{i=1,\dots,|P|}, \quad F = (f(p_i))_{i=1,\dots,|P|} \in \mathbb{R}^K$$

denotes the regression error.

Proof. We shorten $A = A_{m,n,p}$. Due to Theorem 6.1(iv), R_{A,P_0} has full rank $R_{A,P_0} = |P_0|$. While the nodes P_A are unisolvent with respect to Π_A the interpolation operator

$$I_{P_A} : C^0(\Omega, \mathbb{R}) \rightarrow \Pi_A, \quad f \mapsto Q_{f,A}$$

is a linear operator with operator norm

$$\|I_{P_A}\| = \sup_{f \in C^0(\Omega, \mathbb{R}), \|f\|_{C^0(\Omega)} \leq 1} \|Q_{f,A}\|_{C^0(\Omega)} = \Lambda(P_A)$$

given by the Lebesgue constant from Definition 7.1. In particular, $I_{P_A}(Q) = Q$ holds for all polynomials $Q \in \Pi_A$. Denote with $Q_I = (Q_{f,A}(p))_{p \in P}$ the values of the interpolant in the data points P and observe that the values of $Q_{f,P_0,A}$ in the interpolation nodes P_A are given by $(Q_{f,P_0,A}(p_\alpha))_{\alpha \in A} \in \mathbb{R}^{|A|} = S_{A,P} \tilde{F}$. Then we deduce:

$$\begin{aligned} \|f - Q_{f,P_0,A}\|_{C^0(M)} &\leq \|f - Q_{f,A}\|_{C^0(\Omega)} + \|Q_{f,A} - Q_{f,P_0,A}\|_{C^0(\Omega)} \\ &\leq \|f - Q_{f,A}\|_{C^0(\Omega)} + \|I_{P_A}(Q_{f,A} - Q_{f,P_0,A})\|_{C^0(\Omega)} \\ &\leq \|f - Q_{f,A}\|_{C^0(\Omega)} + \Lambda(P_A) \|S_{A,P}(Q_I - \tilde{F})\|_\infty \\ &\leq \|f - Q_{f,A}\|_{C^0(\Omega)} + \Lambda(P_A) \|S_{A,P}\|_\infty (\|F - Q_I\|_\infty + \|F - \tilde{F}\|_\infty) \\ &\leq (1 + \Lambda(P_A) \|S_{A,P}\|_\infty) \|f - Q_{f,A}\|_{C^0(\Omega)} + \mu \Lambda(P_A) \|S_{A,P}\|_\infty, \end{aligned}$$

where we used $\|F - Q_I\|_\infty \leq \|f - Q_{f,A}\|_{C^0(\Omega)}$ for the last estimate. \square

The statement implies the following consequence:

COROLLARY 7.3. *Let $m, n, p \in \mathbb{N}$, $A = A_{m,n,p} \subseteq \mathbb{N}^m$ be a downward closed set of multi-indices, $P_A \subseteq \Omega$ be a set of unisolvent nodes satisfying (A1) from Definition 4.1 in dimension $m = 3$. Given are a closed smooth surface $S \subseteq \mathbb{R}^3$, a regular point set $P_n = \{p_0, \dots, p_{K_n}\} \subseteq S$, $K_n \geq |A_{m,n,p}|$, and a continuous function $f : S \rightarrow \mathbb{R}$ possessing an (analytic) extension to a function $\tilde{f} : \Omega \rightarrow \mathbb{R}$ such that*

$$(7.3) \quad \|\tilde{f} - Q_{\tilde{f}, A_{m,n,p}}\|_{C^0(\Omega)} = o(1 + \Lambda(P_{m,n,p}) \|S_{A_{m,n,p}, P_n}\|_\infty).$$

Given that the regression error μ from Theorem 7.2 tends to zero fast, $\mu \in o(\Lambda(P_A) \|S_{A,P}\|_\infty)$, the sequence of polynomial interpolants $Q_{f, P_{0,n}, A_{m,n,p}}$ from Theorem 6.1(i) approximate f , i.e.,

$$Q_{f, P_{0,n}, A_{m,n,p}} \xrightarrow{n \rightarrow \infty} f \quad \text{uniformly on } S.$$

Proof. The proof follows from Theorem 7.2. \square

While the choice of Leja-ordered Chebyshev-Lobatto nodes, (A2) in Definition 4.1, results in small Lebesgue constants $\Lambda(P_{m,n,p})$ [32], the question of which functions $f : S \rightarrow \mathbb{R}$ can be expected to satisfy the condition in Eq. (7.3) remains. To answer this question, we first summarise recent results by [3, 79] that provide a deeper insight:

Let E_{m,h^2}^2 be the *Newton ellipse* with foci 0 and m and leftmost point $-h^2$. For $m \in \mathbb{N}$ and $h \in [0, 1]$, we set $\rho = h + \sqrt{1 + h^2}$ and call the open region

$$(7.4) \quad N_{m,\rho} = \left\{ (z_1, \dots, z_m) \in \mathbb{C}^m : (z_1^2 + \dots + z_m^2) \in E_{m,h^2}^2 \right\}$$

the *Trefethen domain* [79]. We call a continuous function $f : \Omega \rightarrow \mathbb{R}$ a *Trefethen function* if $f = \sum_{\alpha \in \mathbb{N}^m} c_\alpha \prod T_{\alpha_i} \in \Pi_{A_{m,n,p}}$ can be expanded in an absolute convergent Chebyshev series on Ω and in addition can be *analytically extended* to the Trefethen domain $N_{m,\rho} \subseteq \mathbb{C}^m$ of radius $\rho > 1$. In [79] Trefethen proved an upper bound on the convergence rate for truncating the Trefethen function $\mathcal{T}_{A_{m,n,p}}(f) = \sum_{\alpha \in A_{m,n,p}} c_\alpha \prod T_{\alpha_i} \in \Pi_{A_{m,n,p}}$ to the polynomial space $\Pi_{A_{m,n,p}}$:

$$(7.5) \quad \|f - \mathcal{T}_{A_{m,n,p}}(f)\|_{C^0(\Omega)} = \begin{cases} \mathcal{O}_\varepsilon(\rho^{-n/\sqrt{m}}) & p = 1 \\ \mathcal{O}_\varepsilon(\rho^{-n}) & p = 2 \\ \mathcal{O}_\varepsilon(\rho^{-n}) & p = \infty, \end{cases}$$

where $g \in \mathcal{O}_\varepsilon(\rho^{-n})$ if and only if $g \in \mathcal{O}((\rho - \varepsilon)^{-n}) \forall \varepsilon > 0$.

This suggests that interpolation or regression with respect to *Euclidean l_2 -degree* or *maximum l_∞ -degree* can achieve faster convergence rates than interpolation with respect to *total l_1 -degree*, with l_2 -degree requiring less coefficients than l_∞ -degree, see Eq. (3.1). If f is a (relaxed) signed distance function, as in section 6.2, we therefore find the following consequence of Corollary 7.3:

Remark 7.4. Given a surface $S \subseteq \Omega$ and a regular point set $P \subseteq S$, assume there exists a smooth relaxed signed distance function $d : \Omega \supseteq S \rightarrow \mathbb{R}$, which in addition also is a Trefethen function for which the optimal (Euclidean) rate in Eq. (7.5) applies with radius $\rho > 1$. Thus:

$$(7.6) \quad \|d - Q_{d, A_{3,n,2}}\|_{C^0(\Omega)} \in \mathcal{O}(\rho^{-n}) \quad \text{and} \quad \rho^{-n} \in o(1 + \Lambda(P_{3,n,p}) \|S_{A_{3,n,p}, P}\|_\infty).$$

Then, the surface $S \approx Q_{d, A_{3,n,2}}^{-1}(0)$ can be uniformly approximated by fitting d according to Eq. (6.11).

Because Trefethen functions are a general class of analytic functions [79], the numerical experiments in Section 9.4 suggest that Eq. (7.6) holds for a larger set of smooth closed surfaces S .

8. Curvatures and differential operators on polynomial hypersurfaces. Once a GPLS approximation of a surface has been determined, differential geometric quantities can be computed analytically. We provide explicit formulas for computing mean curvature, Gauss curvature, and the Laplacian of mean curvature.

We consider the affine algebraic variety $M \subseteq \mathbb{R}^3$ as an iso-hypersurface of a GPLS $Q_M^{-1}(0) = M$, as in Theorem 6.1. In order to provide explicit formulas for basic geometric quantities of M , we follow [25] in \mathbb{R}^3 with standard inner product $\langle e_i, e_j \rangle = \delta_{i,j}$ and standard basis $\{e_i\}_{i=1,\dots,3}$.

8.1. Mean and Gauss curvature. The *gradient* $\nabla Q_M = (\partial_x Q_M, \partial_y Q_M, \partial_z Q_M) \in \mathbb{R}^3$ and the *Hessian* $H_M = \nabla(\nabla Q_M) \in \mathbb{R}^{3 \times 3}$ of Q_M

$$H_M = \begin{pmatrix} \frac{\partial^2 Q_M}{\partial_x^2} & \frac{\partial^2 Q_M}{\partial_x \partial_y} & \frac{\partial^2 Q_M}{\partial_x \partial_z} \\ \frac{\partial^2 Q_M}{\partial_y \partial_x} & \frac{\partial^2 Q_M}{\partial_y^2} & \frac{\partial^2 Q_M}{\partial_y \partial_z} \\ \frac{\partial^2 Q_M}{\partial_z \partial_x} & \frac{\partial^2 Q_M}{\partial_z \partial_y} & \frac{\partial^2 Q_M}{\partial_z^2} \end{pmatrix}$$

are the main ingredients for the following computations. Both Gauss and mean curvature can be computed from these quantities [25] as:

$$(8.1) \quad K_{\text{Gauss}} = \frac{\det \begin{pmatrix} H_M & \nabla Q_M^T \\ \nabla Q_M^T & 0 \end{pmatrix}}{\|\nabla Q_M\|^4}$$

$$(8.2) \quad K_{\text{mean}} = \frac{\nabla Q_M H_M \nabla Q_M^T - \|\nabla Q_M\|^2 \text{trace}(H_M)}{2\|\nabla Q_M\|^3}.$$

While there are several alternative formulas [25], the above two allow for stable and numerically accurate evaluation, as we demonstrate in Section 9.2.

8.2. The Laplacian of mean curvature. The algebraic variety $M = Q_M^{-1}(0)$ of the GPLS, together with its unit normal field $\eta = \nabla Q_M / \|\nabla Q_M\|$, enables computing covariant derivatives and, therefore, the surface-intrinsic gradient and the *Laplace-Beltrami operator* of a function $f : M \rightarrow \mathbb{R}$ as:

$$\begin{aligned} \nabla_M f &= \nabla f - \langle \eta, \nabla f \rangle \eta \\ \Delta_M f &= \Delta f + 2K_{\text{mean}} \langle \eta, \nabla f \rangle - \langle \eta, \nabla^2 f \cdot \eta \rangle, \end{aligned}$$

where $\nabla^2 f$ denotes the Jacobian of the gradient of f [58, 82].

Computing the intrinsic Laplacian of mean curvature, a 4th-order differential term of the surface, is required in many applications, including surface diffusion [28, 67, 71, 74], and turns out to mostly be the bottleneck in terms of accuracy and runtime performance. For a GPLS $M = Q_M^{-1}(0)$ with unit normal field $\eta = \nabla Q_M / \|\nabla Q_M\|$, an analytical identity can be derived by splitting the formula for mean curvature into two parts

$$K_{\text{mean}} = \frac{1}{2} (\nabla Q_M H_M \nabla Q_M^T - \|\nabla Q_M\|^2 \text{trace}(H_M)) \cdot \frac{1}{\|\nabla Q_M\|^3} =: u \cdot v$$

and computing:

$$(8.3) \quad \begin{aligned} \Delta_M K_{\text{mean}} &= \Delta(uv) + 2K_{\text{mean}} \langle \eta, \nabla(uv) \rangle - \langle \eta, \nabla^2(uv) \eta \rangle \\ &= u\Delta v + 2 \langle \nabla u, \nabla v \rangle + v\Delta u + 2(uv) \langle \eta, u\nabla v + v\nabla u \rangle \\ &\quad - \langle \eta, (u\nabla^2 v + \nabla u \otimes \nabla v + \nabla v \otimes \nabla u + v\nabla^2 u) \eta \rangle. \end{aligned}$$

Numerical experiments involving these computations are shown in section 9.3.

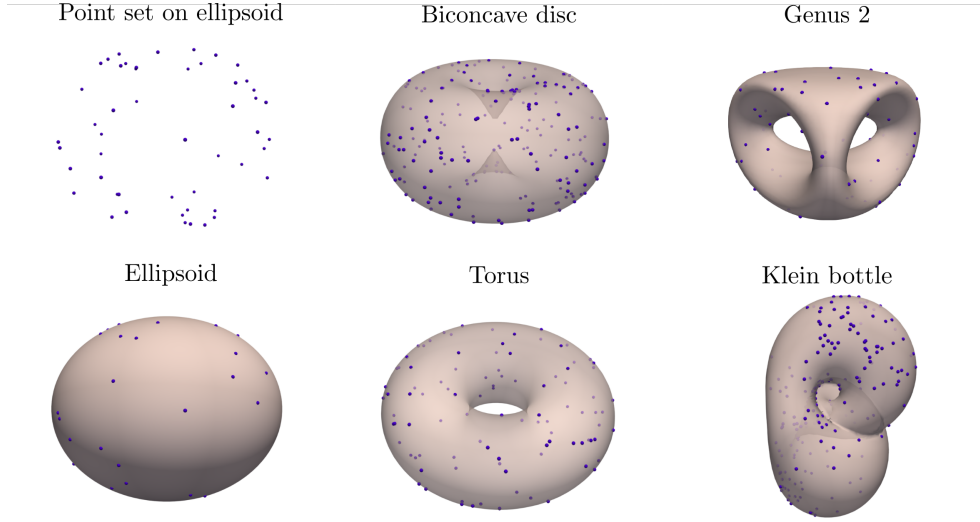


FIG. 1. The GPLS $Q_M^{-1}(0)$ derived from randomly sampled points (blue dots) on the five algebraic test surfaces (S1)–(S5).

9. Numerical Experiments. We implemented the present GPLS approach based on Theorem 6.1 in Python as part of the package MINTERPY [35]. In the following numerical experiments, we benchmark our implementation in comparison with two related alternative methods:

- B1) Curved Finite Elements (CFE): This method uses a *polygonal surface mesh* and curved finite elements to locally approximate the surface for each mesh element with a polynomial of degree 7. The method is implemented using DUNE 2.7.0 [61].
- B2) Closest-Point Finite Differences (CP-FD): This method combines the *closest-point extension* of a *level set* with local finite-difference stencils for polynomial interpolation [64]. The method is implemented using OPENFPM [37].

All numerical experiments were run on a standard Linux laptop (Intel(R) Core(TM) i7-1065G7 CPU @1.30GHz, 32 GB RAM) within reasonable time (seconds up to several minutes). Unless specified otherwise, we use the nodes $P_{A_{3,n,2}} \subseteq \Omega$, $n \in \mathbb{N}$, $p = 2$, which fulfil (A2) from Definition 4.1.

9.1. Approximation of algebraic varieties. We start by comparing the three methods on the basic task of approximating several classic affine algebraic varieties $M \subseteq \mathbb{R}^3$ as given by the following (global) parametrisations:

- S1) Ellipsoid $\frac{x^2}{a^2} + \frac{y^2}{b^2} + \frac{z^2}{c^2} = 1$, $a, b, c \in \mathbb{R} \setminus \{0\}$.
- S2) Biconcave disc $(d^2 + x^2 + y^2 + z^2)^3 - 8d^2(y^2 + z^2) - c^4 = 0$, $c < d \in \mathbb{R} \setminus \{0\}$.
- S3) Torus $(x^2 + y^2 + z^2 + R^2 - r^2)^2 - 4R^2(x^2 + y^2) = 0$, $0 < r < R \in \mathbb{R}$
- S4) Genus 2 surface $2y(y^2 - 3x^2)(1 - z^2) + (x^2 + y^2)^2 - (9z^2 - 1)(1 - z^2) = 0$
- S5) Klein bottle $(x^2 + y^2 + z^2 + 2y - 1)((x^2 + y^2 + z^2 - 2y - 1)^2 - 8z^2) + 16xz(x^2 + y^2 + z^2 - 2y - 1) = 0$.

EXPERIMENT 1 (Surface reconstruction from regular point sets). We sample $N \in \mathbb{N}$ random points $P \subseteq S$, $|P| = N$, on each surface $S = M$ given by the algebraic varieties above,

2D surface	L_∞ error		N
	surface fitting	coefficients	
Ellipsoid ($a = 0.8, b = 0.9, c = 1.0$)	$8.96 \cdot 10^{-16}$	$2.52 \cdot 10^{-15}$	50
Biconcave disc ($d = 0.5, c = 0.375$)	$9.90 \cdot 10^{-15}$	$3.31 \cdot 10^{-6}$	200
Torus ($R = 0.5, r = 0.3$)	$1.13 \cdot 10^{-14}$	$1.05 \cdot 10^{-12}$	100
Genus 2 surface	$1.19 \cdot 10^{-14}$	$2.60 \cdot 10^{-11}$	100
Klein bottle	$1.95 \cdot 10^{-12}$	$1.58 \cdot 10^{-9}$	200

TABLE 1

Reconstruction errors for the GPLS method with different numbers of uniformly random surface points N on the 2D surfaces given by the algebraic varieties shown in Fig. 1.

as visualised in Fig. 1. All point positions are stored with machine precision (32-bit double-precision arithmetics), i.e., the formulas above hold for all $q \in P$ with an accuracy of $\approx 10^{-15}$.

When considering the multi-indices $A_{3,n,2}$ with $n = \deg(M) \in \mathbb{N}$ equal to the degree of the corresponding variety, then Corollary 6.4(i) applies to all algebraic varieties, allowing us to compute the polynomial $Q_M \in \Pi_A$ with $M = Q_M^{-1}(0)$ using the GPLS method with the surface points P . The quality of the GPLS approximation is measured for each true surface point $q \in P$ by computing the shortest distance $\text{dist}(q, M) \in \mathbb{R}^+$ to the GPLS surface when following the GPLS normal $\eta(x) = \nabla Q_M(x) / \|\nabla Q_M(x)\|$ due to classic Newton-gradient-descent till reaching $Q_M(q + d_q \eta(q)) = 0$ (with machine precision).

The L_∞ -norm across all surface points and the number of points used (N) are reported in Table 1 (columns “surface fitting” and “ N ”). We observe that the GPLS method approximates all surfaces, including the non-orientable, self-intersecting Klein bottle, with an accuracy close to machine precision. Several repetitions of the experiment for different samples of random surface points produced comparable results differing in accuracy by less than one order of magnitude. The same is true when measuring the fitting error on 100 randomly sampled test points $P_{\text{test}} \subseteq S \setminus P$ that were not used for computing the GPLS.

EXPERIMENT 2 (Coefficients reconstruction). We consider the GPLS $Q_M \in \Pi_A$ from Experiment 1 in canonical form $Q_M = \sum_{\alpha \in A_{3,n,2}} d_\alpha x^\alpha$ and normalise $\tilde{Q}_M = \lambda Q_M$ with $\lambda \in \mathbb{R}$ so that the leading coefficient $d_\alpha \in \mathbb{R}$, $\alpha = \text{argmax}_{\alpha \in A_{3,n,2}} \{d_\alpha \neq 0\}$ coincides with the leading coefficient c_α of the original surface parametrisation polynomial Q_S , $S = (S1), \dots, (S5)$ in canonical form. According to Corollary 6.4(i), the two polynomials have to be identical, i.e., $\tilde{Q}_M = Q_S$. The L_∞ difference $\|D - C\|_\infty$, $D = (d_\alpha)_{\alpha \in A_{3,n,2}}$, $C = (c_\alpha)_{\alpha \in A_{3,n,2}}$, of the GPLS and ground-truth coefficients is reported in Table 1 (column “coefficients”).

Apart from the biconcave disc, all polynomial formulas are recovered close to machine precision. The lower accuracy reached for the biconcave disc reflects its relatively high polynomial degree $n = 6$, which makes representations in canonical polynomial basis imprecise.

Together, the results of Experiments 1 and 2 validate the GPLS method for computing global level-set surface approximations from regular point samples on (low-degree) algebraic surfaces.

9.2. Mean and Gauss curvatures of algebraic varieties. After having validated the surface approximation properties of the GPLS method, we test how accurately differential geometric quantities of the surface can be computed from the GPLS parametrisation. We first consider Gauss and mean curvature, which are 2nd-order derivatives, before looking at the 4th-order Laplacian of curvature in the subsequent section.

For ellipsoids and tori, the analytical expressions are known:

Global Polynomial Level Set (GPLS)	L_∞ curvature error		N
	K_{mean}	K_{Gauss}	
Ellipsoid ($a = 1.0, b = 1.0, c = 1.0$)	$1.78 \cdot 10^{-15}$	$3.55 \cdot 10^{-15}$	50
Ellipsoid ($a = 1.0, b = 1.0, c = 0.6$)	$1.78 \cdot 10^{-15}$	$5.77 \cdot 10^{-15}$	50
Ellipsoid ($a = 0.6, b = 0.6, c = 1.0$)	$3.33 \cdot 10^{-15}$	$1.24 \cdot 10^{-14}$	50
Ellipsoid ($a = 0.6, b = 0.8, c = 1.0$)	$3.11 \cdot 10^{-15}$	$7.11 \cdot 10^{-15}$	50
Biconcave disc ($d = 0.5, c = 0.375$)	$1.46 \cdot 10^{-10}$	$6.38 \cdot 10^{-10}$	200
Biconcave disc ($d = 0.5, c = 0.4$)	$5.21 \cdot 10^{-11}$	$2.42 \cdot 10^{-10}$	200
Biconcave disc ($d = 0.4, c = 0.2$)	$9.24 \cdot 10^{-11}$	$7.78 \cdot 10^{-11}$	200
Torus ($R = 0.5, r = 0.3$)	$3.69 \cdot 10^{-13}$	$2.21 \cdot 10^{-12}$	100
Torus ($R = 0.4, r = 0.3$)	$4.89 \cdot 10^{-13}$	$6.73 \cdot 10^{-12}$	100
Torus ($R = 0.5, r = 0.1$)	$4.70 \cdot 10^{-12}$	$1.71 \cdot 10^{-11}$	100
Genus 2 surface	$9.40 \cdot 10^{-13}$	$3.46 \cdot 10^{-12}$	100
Curved Finite Elements (CFE)			
Ellipsoid ($a = 1.0, b = 1.0, c = 1.0$)	$2.23 \cdot 10^{-7}$	-	54722
Ellipsoid ($a = 1.0, b = 1.0, c = 0.6$)	$8.66 \cdot 10^{-7}$	-	46082
Ellipsoid ($a = 0.6, b = 0.6, c = 1.0$)	$1.07 \cdot 10^{-7}$	-	46082
Ellipsoid ($a = 0.6, b = 0.8, c = 1.0$)	$3.57 \cdot 10^{-7}$	-	46082
Torus ($R = 0.5, r = 0.3$)	$8.7 \cdot 10^{-7}$	-	463680
Torus ($R = 0.4, r = 0.3$)	$5.29 \cdot 10^{-7}$	-	124800
Torus ($R = 0.5, r = 0.1$)	$4.06 \cdot 10^{-6}$	-	79680
Closest-Point Finite Differences (CP-FD)			
Ellipsoid ($a = 1.0, b = 1.0, c = 1.0$)	$1.31 \cdot 10^{-7}$	$2.63 \cdot 10^{-7}$	725912
Ellipsoid ($a = 1.0, b = 1.0, c = 0.6$)	$2.45 \cdot 10^{-5}$	$6.16 \cdot 10^{-5}$	543632
Ellipsoid ($a = 0.6, b = 0.6, c = 1.0$)	$3.55 \cdot 10^{-5}$	$1.93 \cdot 10^{-4}$	383600
Ellipsoid ($a = 0.6, b = 0.8, c = 1.0$)	$2.10 \cdot 10^{-5}$	$6.85 \cdot 10^{-5}$	461664
Torus ($R = 0.5, r = 0.3$)	$4.82 \cdot 10^{-5}$	$2.96 \cdot 10^{-4}$	770080
Torus ($R = 0.4, r = 0.3$)	$1.28 \cdot 10^{-3}$	$9.55 \cdot 10^{-3}$	616176
Torus ($R = 0.5, r = 0.1$)	$1.74 \cdot 10^{-3}$	$1.08 \cdot 10^{-2}$	257056

TABLE 2

Errors of curvature computations using the three methods (GPLS, CFE, CP-FD) for orientable algebraic surfaces represented using different numbers of points N .

$$\text{S1) Ellipsoid} \quad K_{\text{mean}} = \frac{|x^2+y^2+z^2-a^2-b^2-c^2|}{2(abc)^2 \left(\frac{x^2}{a^4} + \frac{y^2}{b^4} + \frac{z^2}{c^4}\right)^{3/2}} \quad \text{and} \quad K_{\text{Gauss}} = \frac{1}{(abc)^2 \left(\frac{x^2}{a^4} + \frac{y^2}{b^4} + \frac{z^2}{c^4}\right)^2}.$$

$$\text{S3) Torus} \quad K_{\text{mean}} = \frac{R+2r\cos\theta}{2r(R+r\cos\theta)} \quad \text{and} \quad K_{\text{Gauss}} = \frac{\cos\theta}{r(R+r\cos\theta)}, \quad \text{where we used toric coordinates } (x, y, z) = (R+r\cos\theta)\cos\varphi, (R+r\cos\theta)\sin\varphi, r\sin\theta), \varphi, \theta \in [0, 2\pi).$$

Analytic expressions for the biconcave disc and the genus 2 surface also exist. However, for the sake of simplicity, we used MATHEMATICA 11.3 for the ground-truth computations in these cases.

EXPERIMENT 3 (Curvature computation). *We consider only the orientable surfaces from Experiment 1 and compute their mean and Gauss curvatures from the GPLS approximation according to Eqs. (8.1) and (8.2). We compare the results with those computed using the CFE and CP-FD methods. While GPLS can compute the curvatures once Q_M is determined, CFE*

	L_∞ error	N
Global Polynomial Level Set (GPLS)		
	$\Delta_M K_{\text{mean}}$	
Ellipsoid ($a = 1.0, b = 1.0, c = 1.0$)	$2.09 \cdot 10^{-11}$	50
Ellipsoid ($a = 1.0, b = 1.0, c = 0.6$)	$4.93 \cdot 10^{-11}$	50
Ellipsoid ($a = 0.6, b = 0.6, c = 1.0$)	$8.08 \cdot 10^{-11}$	50
Closest-Point Finite Differences (CP-FD)		
Ellipsoid ($a = 1.0, b = 1.0, c = 1.0$)	$1.18 \cdot 10^{-3}$	725912
Ellipsoid ($a = 1.0, b = 1.0, c = 0.6$)	$1.59 \cdot 10^{-1}$	543632
Ellipsoid ($a = 0.6, b = 0.6, c = 1.0$)	$3.00 \cdot 10^{-1}$	383600

TABLE 3

Maximum errors of the Laplacian of mean curvature $\Delta_M K_{\text{mean}}$ computed using GPLS and CP-FD for axisymmetric ellipsoids.

and CP-FD rely on feasible computational meshes or grids. Some of the benchmark computations for those methods therefore had to be skipped due to incommensurate implementation effort. Curvature errors are measured at each surface/grid point and the L_∞ norm reported in Table 2 along with the total number of surface/grid points N used by the methods.

The curvatures computed by GPLS are seven to eight orders of magnitude more accurate than those computed using either CFE or CP-FD methods. In some cases, the GPLS reaches machine precision. The computational cost in terms of the number of points N required is also orders of magnitude better for GPLS than for CFE and CP-FD.

Moreover, GPLS is the only method that allows evaluating curvature formulae at any location $x_0 \in M$. This allows us to compute the GPLS errors at the points used by CFE and CP-FD, respectively. The resulting GPLS accuracies deviate by less than an order of magnitude from those reported in Table 2 on the points used to derive the GPLS.

9.3. Laplacian of mean curvature. Next, we consider computing a 4th-order differential quantity of the surfaces, the Laplacian of mean curvature. The reference values for axisymmetric ellipsoidal surfaces (with $a = b$) were computed using MATHEMATICA 11.3.

EXPERIMENT 4 (Laplacian of mean curvature). *We compute the surface Laplacian $\Delta_M K_{\text{mean}}$ of the mean curvature using Eq. (8.3) for a GPLS. While Gauss curvature depends non-linearly on the Hessian, Eq. (8.1) computing this quantity using CFE is not straightforward, which is why a direct comparison is omitted. The results computed using the CP-FD and GPLS methods are reported in Table 3.*

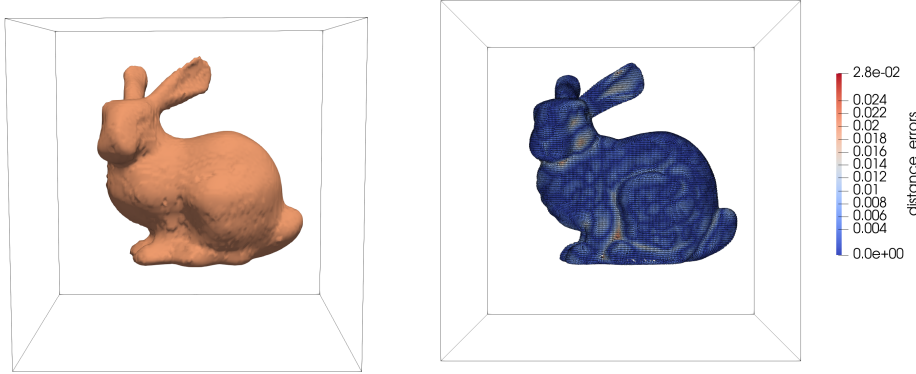
Also for the Laplacian of mean curvature, the GPLS results are orders of magnitude more accurate than the CP-FD ones, while using much fewer surface points. However, both methods lose about 4 orders of magnitude in precision compared to computing mean curvature alone (cf. Table 2, where the same surfaces were considered).

9.4. Non-algebraic surfaces. In order to test the GPLS approach on non-algebraic surfaces, we consider the well-known example surface S_B given by the *Stanford Bunny* dataset¹ containing 35,947 surface points with associated surface-normal vectors. Fig. 2. We complement our investigations by considering the *Spot dataset*², Fig. 3.

EXPERIMENT 5 (Non-Algebraic surface). *We repeat Experiment 1 for the Stanford*

¹available from <http://graphics.stanford.edu/data/3Dscanrep/>

²available from <https://www.cs.cmu.edu/~kmc crane/Projects/ModelRepository/>



PARAVIEW's iso-surface of the GPLS *Stanford Bunny*³ with GPLS distance error

FIG. 2. The GPLS approximation of the Stanford Bunny dataset. Left: visualisation of the level set $Q_M^{-1}(0)$ for l_2 -degree $n=9$ derived from 4000 surface points. Right: The entire dataset with all 35.947 surface points with color corresponding to the closest point distance to the GPLS.

Bunny S_B and the Spot surface S_C , for which Corollary 6.4(i) does not apply. Therefore, we sub-sample 4000 points P and their normals $\eta(q)$, $q \in P$, uniform at random. By moving the points along the dataset normals $q' = q + \lambda \eta(q)$, $\lambda = \pm 0.005, \pm 0.01, \pm 0.035$, we generate a surrounding narrow band with (relaxed) signed distance function $d(q') = \lambda$. The GPLS Q_M is derived by fitting d according to section 6.2. The GPLS quality is measured by computing the shortest distances $\text{dist}(q, M) \in \mathbb{R}^+$ across the entire dataset $q \in P$ as in Experiment 1. The maximum and mean errors (distances) $E_\infty / E_{\text{mean}}$ are listed in Tables 4,5 for different choices of polynomial degree and l_p -degree.

For both datasets the lowest distance error (in bold) is reached for Euclidean l_2 -degree, reflecting the discussion in Section 7, Remark 7.4 and [79] on the optimality of that choice. Fig. 2(left) and Fig. 3(left) show the surface visualised from the most accurate GPLS using PARAVIEW's iso-surface rendering. The colorbar plots in Fig. 2(right), Fig. 3(left) indicate the distance errors of the GPLS to the original datasets, respectively. For the Stanford bunny the GPLS requires $|C| = 486$ polynomial coefficients, $C \in \mathbb{R}^{[A_{3,9,2}]}$, hence delivering a representation of S_B with a compression ratio $r = 35.947/486 \approx 74$. For the Spot dataset $|C| = 847$ polynomial coefficients are required, $C \in \mathbb{R}^{[A_{3,12,2}]}$, yielding compression ratio $r = 5856/847 = 7$. Regarding the results, we expect that the shown examples are at the limit of what the GPLS method can handle in terms of geometric complexity.

degree n	$E_\infty / E_{\text{mean}}, p=1$	$E_\infty / E_{\text{mean}}, p=2$	$E_\infty / E_{\text{mean}}, p=\infty$
7	0.418 / 0.006	0.075 / 0.004	0.035 / 0.003
8	0.143 / 0.005	0.054 / 0.003	0.055 / 0.003
9	0.102 / 0.004	0.029 / 0.003	0.070 / 0.002
10	0.043 / 0.004	0.049 / 0.003	0.167 / 0.002
11	0.068 / 0.003	0.022 / 0.001	0.160 / 0.002

TABLE 4

Maximum fitting (distance) errors for GPLS approximations of the Stanford Bunny surface with various polynomial degrees n and l_p -degrees p . The best fit is highlighted in bold.

Given the GPLS approximation of the Stanford Bunny surface S_B , we next address the

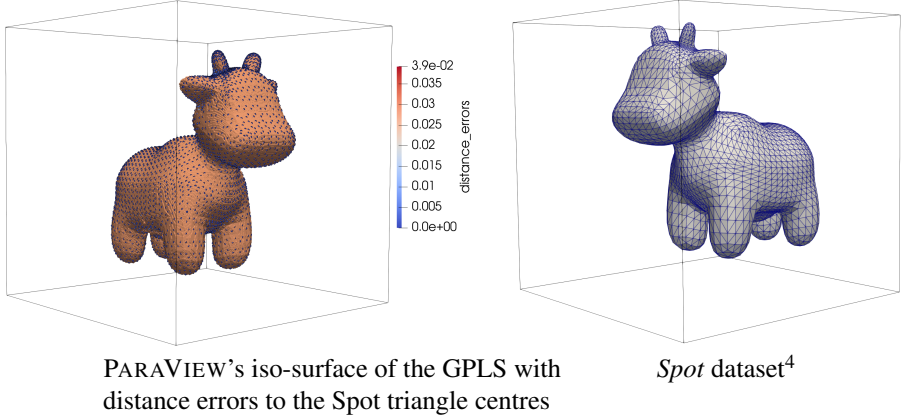


FIG. 3. The GPLS approximation of the Spot dataset. Left: PARAVIEW’s isocontour visualization of the level set $Q_M^{-1}(0)$ for l_2 -degree $n = 12$ derived from 4000 surface points with color corresponding to the closest point distance to the original Spot dataset (visualised as points). Right: The entire Spot dataset with all 5856 triangles. Triangle centres and their normals are used as data inputs for the GPLS.

degree n	$E_\infty / E_{\text{mean}}, p = 1$	$E_\infty / E_{\text{mean}}, p = 2$	$E_\infty / E_{\text{mean}}, p = \infty$
8	0.099 / 0.005	0.110 / 0.0030	0.055 / 0.0020
9	0.182 / 0.004	0.068 / 0.0010	0.123 / 0.0005
10	0.082 / 0.004	0.063 / 0.0010	0.187 / 0.0020
11	0.085 / 0.003	0.042 / 0.0005	0.036 / 0.0003
12	0.081 / 0.001	0.029 / 0.0003	0.044 / 0.0010

TABLE 5

Maximum fitting (distance) errors for GPLS approximations of the Spot surface with various polynomial degrees n and l_p -degrees p . The best fit is highlighted in bold.

task of globally fitting a scalar function $f : S_B \rightarrow \mathbb{R}$ on the surface.

EXPERIMENT 6 (Function fitting on non-algebraic surface). We sample the Runge function $f(x) = 1/(1 + |x|^2)$ at 10,000 randomly chosen surface points $P \subseteq S_B$ on the Stanford Bunny and apply the multivariate regression scheme from Remark 6.6 to derive approximations $Q_{P,f,A_{3,n,p}} \approx f$ of f on S_B . The L_∞ approximation errors are measured across 500 random surface points not used for the regression and plotted in Fig. 4 as a function of p and n .

All regressions achieve reasonable approximation of the Runge function. Regression with respect to Euclidean and maximum degree ($p = 2, \infty$) convergences faster with degree n than total-degree regression ($p = 1$), confirming the expectations of section 7. However, l_1 regression reaches the overall best approximation. In contrast, $l_{2,\infty}$ regression becomes unstable (for $n > 11$ or $n > 17$, respectively) with maximum degree $p = \infty$ performing worst. Euclidean regression ($p = 2$) reaches a 10^{-7} approximation fastest (for degree $n = 17$), but the specific sample point distribution used here hampers its optimality in terms of coefficient count, as formulated in Corollary 7.3. An extended discussion of these effects is provided by [54, 79], including an explanation for the observed numerical instabilities.

Since the Runge function is highly varying and notoriously hard to interpolate (“Runge’s Phenomenon”), the accuracies reached here suggest that a larger class of functions can be approximated using the present method, supporting classic computational tasks in differential geometry.

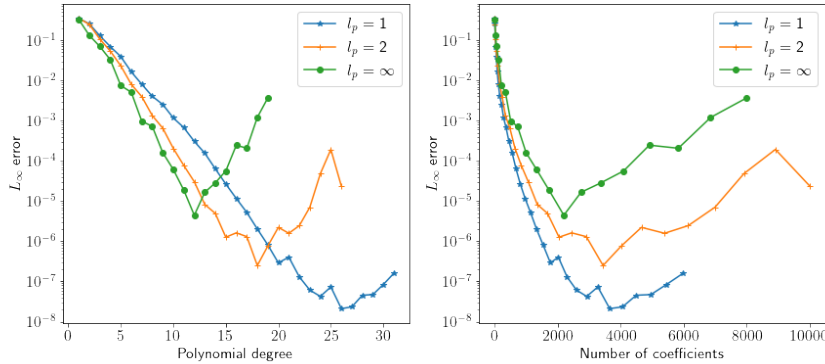


FIG. 4. Maximum approximation errors for fitting the Runge function on the Stanford Bunny from 10,000 uniformly randomly placed surface samples for different polynomial degrees. The total numbers of coefficients are plotted on the right.

10. Conclusion. We have combined basic algebraic geometry and classic numeric analysis to approximate smooth closed surfaces $S \subset \mathbb{R}^3$ by algebraic varieties with global polynomial level set (GPLS) $M = Q_M^{-1}(0) \approx S$. We proved uniqueness of these approximations in Theorem 6.1, with further discussion given in Remark 6.2. We presented numerical experiments of computing differential-geometric quantities (curvatures and Laplacian of curvature) of algebraic surfaces approximated by their GPLS. Both the computational efficiency, in terms of the surface point counts $|P|$, $P \subseteq S$, as well as the accuracy reached by the GPLS method were superior to Curved Finite Elements (CFE) and to Closest-Point Finite Differences (CP-FD) by orders of magnitude.

We then estimated the limitations of GPLS methods in terms of the reachable surface complexity in Theorem 7.2 and numerically demonstrated them in the example of the *Stanford Bunny* and the *Spot dataset*. We then achieved global approximation of the highly varying Runge function on the surface of the Stanford Bunny, suggesting that the presented approach applies to a larger class of surfaces and functions, as for example occurring in *biophysics* [10, 48, 65, 67] or *mechanics* [62, 66].

In the present work, we focused on static surfaces. Our results, however, suggest that the proposed method could also provide a starting point for dynamic surface deformation simulations, potentially providing an alternative to well-established *level set methods and fast marching methods* [70].

We also note that the concept of GPLS is not limited to two-dimensional surfaces, but can be extended to higher-dimensional embedded (hypersurfaces) manifolds $\mathcal{M} \subseteq \mathbb{R}^m$, $m \in \mathbb{N}$. There, the computational efficiency of the GPLS approach in terms of the required number of points $P \subseteq \mathcal{M}$ may pave the way for realising numerical the manifold models required, for instance, for Ricci-DeTurck flow simulations [21].

Acknowledgments. We are deeply grateful for the insights and support we received in discussions with Prof. Oliver Sander (TU Dresden). We want to thank Dan Fortunato (CCM Simons Foundation) for the Spot dataset and fruitful discussions on the subject we had.

References.

- [1] A. BEN-ISRAEL AND T. N. GREVILLE, *Generalized inverses: theory and applications*,

- vol. 15, Springer Science & Business Media, 2003.
- [2] M. BERGER, *Riemannian geometry during the second half of the twentieth century*, American Mathematical Society, 2000.
 - [3] L. BOS AND N. LEVENBERG, *Bernstein–Walsh theory associated to convex bodies and applications to multivariate approximation theory*, *Computational Methods and Function Theory*, 18 (2018), pp. 361–388.
 - [4] L. BRUTMAN, *Lebesgue functions for polynomial interpolation – a survey*, *Annals of Numerical Mathematics*, 4 (1996), pp. 111–128.
 - [5] F. CALAKLI AND G. TAUBIN, *Ssd: Smooth signed distance surface reconstruction*, in *Computer Graphics Forum*, vol. 30, Wiley Online Library, 2011, pp. 1993–2002.
 - [6] J. C. CARR, R. K. BEATSON, J. B. CHERRIE, T. J. MITCHELL, W. R. FRIGHT, B. C. MCCALLUM, AND T. R. EVANS, *Reconstruction and representation of 3D objects with radial basis functions*, *Proceedings of the 28th annual conference on Computer graphics and interactive techniques*, (2001).
 - [7] G. CASCIOLA, D. LAZZARO, L. B. MONTEFUSCO, AND S. MORIGI, *Shape preserving surface reconstruction using locally anisotropic radial basis function interpolants*, *Comput. Math. Appl.*, 51 (2006), pp. 1185–1198.
 - [8] A. CHKIFA, A. COHEN, AND C. SCHWAB, *High-dimensional adaptive sparse polynomial interpolation and applications to parametric pdes*, *Foundations of Computational Mathematics*, 14 (2014), pp. 601–633.
 - [9] A. COHEN AND G. MIGLIORATI, *Multivariate approximation in downward closed polynomial spaces*, in *Contemporary Computational Mathematics-A celebration of the 80th birthday of Ian Sloan*, Springer, 2018, pp. 233–282.
 - [10] H. COLIN-YORK, J. HEDDLESTON, E. WAIT, N. KAREDLA, M. DESANTIS, S. KHUON, T.-L. CHEW, I. F. SBALZARINI, AND M. FRITZSCHE, *Quantifying molecular dynamics within complex cellular morphologies using LLSM-FRAP*, *Small Methods*, (2022), p. 2200149.
 - [11] C. DE BOOR, *Subroutine package for calculating with b-splines.*, tech. report, Los Alamos National Lab.(LANL), Los Alamos, NM (United States), 1971.
 - [12] C. DE BOOR, *A practical guide to splines*, vol. Volume 27, Applied Mathematical Sciences, New York: Springer, 01 1978, <https://doi.org/10.2307/2006241>.
 - [13] C. DE BOOR AND A. RON, *On multivariate polynomial interpolation*, *Constructive Approximation*, 6 (1990), pp. 287–302.
 - [14] C. DE BOOR AND A. RON, *Computational aspects of polynomial interpolation in several variables*, *Mathematics of Computation*, 58 (1992), pp. 705–727.
 - [15] K. DECKELNICK, G. DZIUK, AND C. M. ELLIOTT, *Computation of geometric partial differential equations and mean curvature flow*, *Acta numerica*, 14 (2005), pp. 139–232.
 - [16] J. DIEUDONNÉ AND A. GROTHENDIECK, *Éléments de géométrie algébrique*, Institut des Hautes Études Scientifiques, (1971).
 - [17] G. DZIUK AND C. M. ELLIOTT, *Finite elements on evolving surfaces*, *IMA Journal of Numerical Analysis*, 27 (2007), pp. 262–292, <https://doi.org/10.1093/imanum/drl023>, <https://doi.org/10.1093/imanum/drl023>, <https://arxiv.org/abs/https://academic.oup.com/imajna/article-pdf/27/2/262/1980490/drl023.pdf>.
 - [18] G. DZIUK AND C. M. ELLIOTT, *Finite element methods for surface PDEs*, *Acta Numerica*, 22 (2013), pp. 289–396.
 - [19] C. A. FLETCHER, *Computational galerkin methods*, in *Computational galerkin methods*, Springer, 1984, pp. 72–85.
 - [20] C. A. J. FLETCHER, *Galerkin Finite-Element Methods*, Springer Berlin Heidelberg, Berlin, Heidelberg, 1984, pp. 86–154, https://doi.org/10.1007/978-3-642-85949-6_3, https://doi.org/10.1007/978-3-642-85949-6_3.

- [21] H. FRITZ, *Numerical Ricci–DeTurck flow*, Numerische Mathematik, 131 (2015), pp. 241–271.
- [22] K. F. GAUSS AND P. PESIC, *General investigations of curved surfaces*, Courier Corporation, 2005.
- [23] W. GAUTSCHI, *Numerical analysis*, Springer Science & Business Media, 2011.
- [24] N. A. GERSHENFELD AND N. GERSHENFELD, *The nature of mathematical modeling*, Cambridge university press, 1999.
- [25] R. GOLDMAN, *Curvature formulas for implicit curves and surfaces*, Computer Aided Geometric Design, 22 (2005), pp. 632–658.
- [26] L. GOMES, O. R. P. BELLON, AND L. SILVA, *3D reconstruction methods for digital preservation of cultural heritage: A survey*, Pattern Recognition Letters, 50 (2014), pp. 3–14.
- [27] W. J. GORDON AND R. F. RIESENFELD, *B-spline curves and surfaces*, in Computer Aided Geometric Design, R. E. BARNHILL and R. F. RIESENFELD, eds., Academic Press, 1974, pp. 95–126, <https://doi.org/10.1016/B978-0-12-079050-0.50011-4>, <https://www.sciencedirect.com/science/article/pii/B9780120790500500114>.
- [28] J. B. GREER, A. L. BERTOZZI, AND G. SAPIRO, *Fourth order partial differential equations on general geometries*, Journal of Computational Physics, 216 (2006), pp. 216–246.
- [29] A. HATCHER, *Algebraic topology*, Cambridge University Press, Cambridge, New York, 2002, <http://opac.inria.fr/record=b1122188>. Autre(s) tirage(s) : 2003,2004,2005,2006.
- [30] A. HATCHER, *Vector bundles and k-theory*, <http://www.math.cornell.edu/~hatcher>, (2003).
- [31] M. HECHT, B. L. CHEESEMAN, K. B. HOFFMANN, AND I. F. SBALZARINI, *A quadratic-time algorithm for general multivariate polynomial interpolation*, arXiv preprint arXiv:1710.10846, (2017).
- [32] M. HECHT, K. GONCIARZ, J. MICHELFEIT, V. SIVKIN, AND I. F. SBALZARINI, *Multivariate interpolation in unisolvent nodes—lifting the curse of dimensionality*, arXiv preprint arXiv:2010.10824, (2020).
- [33] M. HECHT, K. B. HOFFMANN, B. L. CHEESEMAN, AND I. F. SBALZARINI, *Multivariate Newton interpolation*, arXiv preprint arXiv:1812.04256, (2018).
- [34] M. HECHT AND I. F. SBALZARINI, *Fast interpolation and Fourier transform in high-dimensional spaces*, in Intelligent Computing. Proc. 2018 IEEE Computing Conf., Vol. 2., K. Arai, S. Kapoor, and R. Bhatia, eds., vol. 857 of Advances in Intelligent Systems and Computing, London, UK, 2018, Springer Nature, pp. 53–75.
- [35] U. HERNANDEZ ACOSTA, S. KRISHNAN THEKKE VEETIL, D. WICAKSONO, AND M. HECHT, *MINTERPY - multivariate interpolation in python*, <https://github.com/casus/minterpy/>, (2021).
- [36] H. HUANG, D. LI, H. ZHANG, U. M. ASCHER, AND D. COHEN-OR, *Consolidation of unorganized point clouds for surface reconstruction*, ACM SIGGRAPH Asia 2009 papers, (2009).
- [37] P. INCARDONA, A. LEO, Y. ZALUZHNYI, R. RAMASWAMY, AND I. F. SBALZARINI, *OpenFPM: A scalable open framework for particle and particle-mesh codes on parallel computers*, Computer Physics Communications, 241 (2019), pp. 155–177.
- [38] J. JOST, *Riemannian geometry and geometric analysis*, Springer, 2008.
- [39] D. KHAN, M. A. SHIRAZI, AND M. Y. KIM, *Single shot laser speckle based 3D acquisition system for medical applications*, Optics and Lasers in Engineering, 105 (2018), pp. 43–53.
- [40] D. M. KROLL AND G. GOMPPER, *The conformation of fluid membranes: Monte Carlo simulations*, Science, 255 (1992), pp. 968–971, <https://doi.org/10.1126/science>.

- 1546294, <https://www.science.org/doi/abs/10.1126/science.1546294>.
- [41] W. KÜHNEL, *Differential geometry: Curves—Surfaces—Manifolds*, American Mathematical Society, 2017.
- [42] F. LEJA, *Sur certaines suites liées aux ensembles plans et leur application à la représentation conforme*, in *Annales Polonici Mathematici*, vol. 1, Instytut Matematyczny Polskiej Akademi Nauk, 1957, pp. 8–13.
- [43] C. B. MACDONALD, J. BRANDMAN, AND S. J. RUUTH, *Solving eigenvalue problems on curved surfaces using the closest point method*, *Journal of Computational Physics*, 230 (2011), pp. 7944–7956.
- [44] C. B. MACDONALD, B. MERRIMAN, AND S. J. RUUTH, *Simple computation of reaction–diffusion processes on point clouds*, *Proceedings of the National Academy of Sciences*, 110 (2013), pp. 9209–9214.
- [45] C. B. MACDONALD AND S. J. RUUTH, *Level set equations on surfaces via the closest point method*, *Journal of Scientific Computing*, 35 (2008), pp. 219–240.
- [46] S. MACLANE, *Some interpretations of abstract linear dependence in terms of projective geometry*, *American Journal of Mathematics*, 58 (1936), pp. 236–240.
- [47] E. MEIJERING, *A chronology of interpolation: From ancient astronomy to modern signal and image processing*, *Proceedings of the IEEE*, 90 (2002), pp. 319–342.
- [48] A. MIETKE, V. JEMSEENA, K. V. KUMAR, I. F. SBALZARINI, AND F. JÜLICHER, *Minimal model of cellular symmetry breaking*, *Physical review letters*, 123 (2019), p. 188101.
- [49] J. MILNOR, *Stasheff, Characteristic classes*, *Ann. of Math. Studies*, 76 (1974).
- [50] S. OSHER AND R. P. FEDKIW, *Level set methods and dynamic implicit surfaces*, vol. 1, Springer New York, 2005.
- [51] S. OSHER AND J. A. SETHIAN, *Fronts propagating with curvature-dependent speed: Algorithms based on hamilton-jacobi formulations*, *Journal of computational physics*, 79 (1988), pp. 12–49.
- [52] A. C. ÖZTIRELI, G. GUENNEBAUD, AND M. H. GROSS, *Feature preserving point set surfaces based on non-linear kernel regression*, *Computer Graphics Forum*, 28 (2009).
- [53] L. PIEGL AND W. TILLER, *The NURBS book*, Springer Science & Business Media, 1996.
- [54] R. B. PLATTE, L. N. TREFETHEN, AND A. B. KUIJLAARS, *Impossibility of fast stable approximation of analytic functions from equispaced samples*, *SIAM review*, 53 (2011), pp. 308–318.
- [55] N. PROVATAS AND K. ELDER, *Phase-field methods in materials science and engineering*, John Wiley & Sons, 2011.
- [56] A. RÄTZ AND A. VOIGT, *A diffuse-interface approximation for surface diffusion including adatoms*, *Nonlinearity*, 20 (2006), p. 177.
- [57] A. RÄTZ AND A. VOIGT, *Pde’s on surfaces—a diffuse interface approach*, *Communications in Mathematical Sciences*, 4 (2006), pp. 575–590.
- [58] R. C. REILLY, *Mean curvature, the Laplacian, and soap bubbles*, *The American Mathematical Monthly*, 89 (1982), pp. 180–198.
- [59] J. RUPPERT, *A Delaunay refinement algorithm for quality 2-dimensional mesh generation*, *Journal of algorithms*, 18 (1995), pp. 548–585.
- [60] S. J. RUUTH AND B. MERRIMAN, *A simple embedding method for solving partial differential equations on surfaces*, *Journal of Computational Physics*, 227 (2008), pp. 1943–1961.
- [61] O. SANDER, *Dune — the distributed and unified numerics environment*, *Lecture Notes in Computational Science and Engineering*, (2020), <https://doi.org/https://doi.org/10.1007/978-3-030-59702-3>.

- [62] O. SANDER, P. NEFF, AND M. BIRSAN, *Numerical treatment of a geometrically non-linear planar Cosserat shell model*, Computational Mechanics, 57 (2016), pp. 817–841.
- [63] A. SARD, *The measure of the critical values of differentiable maps*, Bulletin of the American Mathematical Society, 48 (1942), pp. 883–890.
- [64] R. SAYE, *High-order methods for computing distances to implicitly defined surfaces*, Communications in Applied Mathematics and Computational Science, 9 (2014), pp. 107–141.
- [65] I. F. SBALZARINI, A. HAYER, A. HELENIUS, AND P. KOUMOUTSAKOS, *Simulations of (an)isotropic diffusion on curved biological surfaces*, Biophysical journal, 90 (2006), pp. 878–885.
- [66] L. W. SCHWARTZ AND R. R. ELEY, *Simulation of droplet motion on low-energy and heterogeneous surfaces*, Journal of Colloid and Interface Science, 202 (1998), pp. 173–188.
- [67] U. SEIFERT, *Configurations of fluid membranes and vesicles*, Advances in physics, 46 (1997), pp. 13–137.
- [68] J. A. SETHIAN, *Theory, algorithms, and applications of level set methods for propagating interfaces*, Acta numerica, 5 (1996), pp. 309–395.
- [69] J. A. SETHIAN, *Tracking interfaces with level sets: An “act of violence” helps solve evolving interface problems in geometry, fluid mechanics, robotic navigation and materials sciences*, American Scientist, 85 (1997), pp. 254–263.
- [70] J. A. SETHIAN, *Level set methods and fast marching methods: evolving interfaces in computational geometry, fluid mechanics, computer vision, and materials science*, vol. 3, Cambridge university press, 1999.
- [71] J. A. SETHIAN AND D. CHOPP, *Motion by intrinsic Laplacian of curvature*, Interfaces and Free boundaries, 1 (1999), pp. 107–123.
- [72] J. R. SHEWCHUK, *Delaunay refinement algorithms for triangular mesh generation*, Computational geometry, 22 (2002), pp. 21–74.
- [73] S. SMALE, *An infinite dimensional version of Sard’s theorem*, Amer. J. Math., 87 (1965), pp. 861–866.
- [74] P. SMEREKA, *Semi-implicit level set methods for curvature and surface diffusion motion*, Journal of Scientific Computing, 19 (2003), pp. 439–456.
- [75] J. STOER, R. BULIRSCH, R. H. BARTELS, W. GAUTSCHI, AND C. WITZGALL, *Introduction to numerical analysis*, Texts in applied mathematics, Springer, New York, 2002.
- [76] M. SUSSMAN AND E. FATEMI, *An efficient, interface-preserving level set redistancing algorithm and its application to interfacial incompressible fluid flow*, SIAM Journal on scientific computing, 20 (1999), pp. 1165–1191.
- [77] M. SUSSMAN, E. FATEMI, P. SMEREKA, AND S. OSHER, *An improved level set method for incompressible two-phase flows*, Computers & Fluids, 27 (1998), pp. 663–680.
- [78] G. TAUBIN, *Smooth signed distance surface reconstruction and applications*, In Iberoamerican Congress on Pattern Recognition, Springer, 2012, pp. 38–45.
- [79] L. N. TREFETHEN, *Multivariate polynomial approximation in the hypercube*, Proceedings of the American Mathematical Society, 145 (2017), pp. 4837–4844.
- [80] L. N. TREFETHEN, *Approximation theory and approximation practice*, vol. 164, SIAM, 2019.
- [81] L. N. TREFETHEN AND D. BAU III, *Numerical linear algebra*, vol. 50, SIAM, 1997.
- [82] J.-J. XU AND H.-K. ZHAO, *An Eulerian formulation for solving partial differential equations along a moving interface*, Journal of Scientific Computing, 19 (2003), pp. 573–594.